Malaysian Journal of Analytical Sciences (MJAS)
Published by Malaysian Analytical Sciences Society

EFFECTIVE AND FAST ADSORPTIVE REMOVAL OF COOMASSIE BRILLIANT BLUE G 250 DYE FROM WATER USING Fe_3O_4 MAGNETIC NANOPARTICLES

(Penjerapan Penyingkiran Pewarna Coomassie Brilliant Biru G 250 Secara Berkesan dan Pantas Menggunakan Fe_3O_4 Magnetik Nanopartikel)

Siti Khalijah Mahmad Rozi[1,2*], Nur Atikah Saufi[1], and Nur Atiqah Nabilah Mohammad Rashidi[1]

[1]*Faculty of Chemical Engineering & Technology, Universiti Malaysia Perlis, Kompleks Pusat Pengajian Jejawi 3, 02600 Arau,Perlis, Malaysia*
[2]*Centre of Excellence for Biomass Utilization, Universiti Malaysia Perlis, 02600 Arau, Perlis, Malaysia*

**Correspondence: khalijahrozi@unimap.edu.my*

Received: 29 March 2023; Accepted: 23 July 2023; Published: 22 August 2023

Abstract

Coomassie Brilliant Blue G 250 (CBB G 250) is mainly generated from industrial textile effluent. Due to its non-degradable nature, it is not only environmentally hazardous, but also affect human health, causing irritations of the eye, respiratory or gastrointestinal tract. Therefore, a strategy for treating this colorant is necessary. This research highlights the synthesis of Fe_3O_4 Magnetic nanoparticles (Fe_3O_4 MNPs) as a low-cost adsorbent for removal of CBB G 250 dye from aqueous solutions. Fe_3O_4 MNPs were synthesized using chemical coprecipitation method. Characterization results revealed that the peaks at 537, 3400 and 1604 cm^{-1} in the Fourier Transform Infrared Spectroscopy spectrum represented the Fe-O band, O-H stretching and bending on the Fe_3O4 MNPs surface, respectively. Crystal phase analysis indicated that Fe_3O_4 MNPs has a cubic spinel structure. Morphological analysis showed Fe_3O_4 MNPs are in nano-sized, spherical in shape, and have uniformly distributed particle size. The result from magnetic and surface area analyses demonstrated that Fe_3O_4 MNPs have 63.30 emu g^{-1} saturation magnetization and 123.5 m^2 g^{-1} surface area. Thermal stability analysis showed that adsorbed water and hydroxyl group (6.25%) were lost at temperature below 100 ℃. At temperature between 260 ℃ and 540 ℃, approximately 2.09% weight loss were recorded due to change from magnetite (Fe_3O_4) to maghemite (γ- Fe_2O_3) in crystal phase. Elemental analysis revealed that the Fe_3O_4 MNPs showed 24.50 % of Fe and 75.50 % of O. Following the confirmation of Fe_3O_4 MNPs structure, the impact of various parameters such as adsorbent dosage (0.02-0.14 g), contact time (5-20 minutes), initial concentration (25-100 ppm) and pH (3-10) on the adsorption of CBB G 250 dyes were investigated. Experimental results showed that Fe_3O_4 MNPs achieved 95% removal of CBB G 250 at optimum conditions of 0.12 g dosage, 15 minutes contact time, 50 ppm initial dye concentration and at pH value of 8. Adsorption isotherms and kinetics revealed that the adsorption process using Fe_3O_4 MNPs in this study obeys both Langmuir and Freundlich isotherm and pseudo-second-order kinetic. The results obtained from this study confirmed that Fe_3O_4 MNPs can be used as an adsorbent material for the removal of dye from effluent.

Keywords: Fe_3O_4 magnetic nanoparticles, adsorbents, Coomassie Brilliant Blue G 250, dye removal

Abstrak

Coomassie Brilliant Blue G 250 (CBB G 250) ialah efluen tekstil perindustrian yang kebanyakannya dihasilkan daripada efluen tekstil. Disebabkan sifatnya yang tidak terdegradasi, ia berbahaya kepada alam sekitar dan kesihatan manusia dan membawa kepada kerengsaan mata, saluran pernafasan atau gastrousus. Oleh itu, strategi untuk merawat pewarna ini adalah perlu. Oleh itu, penyelidikan ini mengetengahkan sintesis Magnetik nanopartikel Fe_3O_4 (Fe_3O_4 MNPs) sebagai penjerap kos rendah untuk penyingkiran pewarna CBB G 250 daripada larutan akueus. MNP Fe_3O_4 telah disintesis dengan menggunakan kaedah kopresipitasi kimia. Keputusan pencirian mendedahkan bahawa puncak pada 537, 3400 dan 1604 cm^{-1} dalam spektrum Spektroskopi Inframerah Transformasi Fourier masing-masing mewakili jalur Fe-O, regangan O-H dan lenturan pada permukaan Fe_3O_4 MNPs. Analisis fasa kristal menunjukkan bahawa Fe_3O_4 MNPs mempunyai struktur spinel padu. Analisis morfologi menunjukkan Fe_3O_4 MNPs dalam saiz nano, dalam bentuk sfera, dan mempunyai saiz zarah teragih seragam. Hasil daripada analisis magnet dan kawasan permukaan menunjukkan bahawa Fe_3O_4 MNPs mempunyai 63.30 emu g^{-1} kemagnetan tepu dan 123.5 m^2 g^{-1}, masing-masing. Analisis kestabilan terma menunjukkan bahawa air terjerap dan kumpulan hidroksil (6.25 %) hilang pada suhu di bawah 100 °C. Pada suhu 260 hingga 540 °C, penurunan berat lebih kurang 2.09 % direkodkan hasil daripada perubahan daripada magnetit (Fe_3O_4) kepada maghemit (Ɣ- Fe_2O_3) seperti dalam fasa kristal. Analisis unsur mendedahkan bahawa Fe_3O_4 MNPs masing-masing menunjukkan 24.50% dan 75.50% Fe dan O. Selepas struktur Fe_3O_4 MNPs disahkan, pelbagai parameter seperti kesan dos penjerap (0.02-0.14 g), masa sentuhan (5-20 minit), awal kepekatan (25-100 ppm) dan pH (3-10) pada penjerapan pewarna CBB G 250 telah disiasat. Keputusan eksperimen menunjukkan bahawa Fe_3O_4 MNPs mencapai 95% pada keadaan optimum pada 0.12 g dos, 15 minit masa sentuhan, 50 ppm kepekatan awal dan nilai pH 8. Isoterma dan kinetik penjerapan mendedahkan bahawa proses penjerapan menggunakan Fe_3O_4 MNPs pada kajian ini mematuhi kedua-dua Langmuir dan Freundlich isoterm dan kinetik pseudo-second order, masing-masing. Keputusan yang diperolehi daripada kajian ini mengesahkan bahawa Fe_3O_4 MNPs boleh digunakan sebagai bahan penjerap untuk penyingkiran bahan pewarna daripada efluen.

Kata kunci: magnetik nanopartikel Fe_3O_4, penjerap, Coomassie Brilliant Blue G 250, penyingkiran pewarna

Introduction

One of the biggest and most urgent problem in the modern world is environmental pollution. Textile industries are one of the major polluters not only due to high amounts of water used in manufacturing, but the industry also generate high liquid effluent pollutants. In the textile industry, the largest amount of coloured aqueous waste is disposed through dyeing processes, and not only does it has strong persistent color, but also high biological demand for oxygen (BDO) [1].The presence of these dyes in water causes cancer, toxicity, birth defect and teratogenicity, reducing light penetration into the water and consequently preventing photosynthesis of aquatic plants [2]. Coomassie Brilliant Blue G 250 (CBB G 250) is one of the triphenylmethane dyes used widely in the textile industry. These dyes are hazardous to both the environment and human health because of its non-degradable nature, and causes eye irritations as well as respiratory and gastrointestinal tract irritations. Therefore, it is important to treat these types of dyes [3].

Various techniques are currently being used in order to remove dye effluents that are released into open waters, and this includes coagulation [4], precipitation [5], oxidation-ozonation [6], adsorption [7], ion exchange [8], and biological methods. Adsorption method is considered one of the most promising method due to its flexibility, ease of operation, simple design and high efficiency [8]. It has therefore been used extensively in recent years to treat colours. Common adsorbents such as activated carbon, biochar and graphene oxide have been used previously for the removal of dyeing from wastewater. However, these sorbents have several drawbacks, one of which occur during the separation process, a common issue as these sorbents require centrifugation, a procedure which prolongs analysis time especially when dealing with large sample volume [9]. Thus, it cannot be used extensively for the removal of organic dyes from aqueous environment. Therefore, it is necessary to develop a reliable, easy and rapid adsorbent for efficient treatment of dyeing effluents.

One of the potential adsorbent is magnetic nanoparticle (MNPs). Among the various types of MNPs, iron oxides such as magnetite (Fe_3O_4), maghemite (γ-Fe_2O_3) and hematite (α-Fe_2O_3) are common and attractive options due to their biocompatibility, great saturation magnetization and magnetic susceptibility. The advantages of Magnetite (Fe_3O_4) include the best magnetization among the iron oxides, low price, low toxicity and a high specific surface area. Fe_3O_4 magnetic nanoparticle (Fe_3O_4 MNPs) can also be an adsorbent for remediation of organic dye such as CBB G 250 due to its unique features [10]. Since the use of Fe_3O_4 MNPs is seldom documented for decontamination of CBB G 250 from water environment, it is a good idea to study efficiency of Fe_3O_4 MNPs as an adsorbent for treatment of organic dyes from aqueous environment.

The purpose of this study is to develop Fe_3O_4 magnetic nanoparticles (Fe_3O_4 MNPs) for adsorption of CBB G 250 from aqueous solution. The structure of Fe_3O_4 MNPs was characterized using Fourier Transform Infrared Spectroscopy (FTIR), X-ray Diffraction (XRD), Field Emission Scanning Electron Microscopy (FESEM), Energy Dispersive X-ray Spectroscopy (EDX), Thermogravimetric analysis (TGA), Vibrating Sample Magnetometer (VSM) and Brunauer-Emmett-Teller (BET). After the structures of Fe_3O_4 MNPs were confirmed, it was then used as an adsorbent for treatment of CBB G 250 from aqueous environment. During the application part, the screening of several parameters such as dosage of adsorbent, contact time, initial dye concentration, pH of the solution were performed in order to determine characteristcis that influence the efficiency of Fe_3O_4 MNPs to adsorb CBB G 250. Widely-used models were described and analyzed to evaluate the best theoretical adsorption capacity such as adsorption kinetic (pseudo-first, second order and intraparticle diffusion) as well as some isotherm models (Langmuir and Freundlich). The regeneration performance of the Fe_3O_4 MNPs was also examined in six consecutive cycles.

Materials and methods

Chemicals

Iron (III) chloride hexahydrate, iron (II) chloride tetrahydrate and aqueous ammonia were purchased from Fluka Analytical (Germany). The standard for Coomassie Brilliant Blue G 250 (CBB G 250) was obtained from Supelco (Belleffonte, USA). The stock solutions of CBB G 250 dye were prepared in distilled water at 100 ppm. All stock solutions were kept at 4 ^oC.

Instrumentation

The functional groups of the synthesized nanoparticles were first characterized using a FTIR spectrometer (Spectrum 400 PerkinElmer) with a diamond ATR accessory, absorption mode with 4 scans at a resolution of ±4 cm^{-1}, and a wavenumber range of 4000 to 450 cm^{-1}. FESEM images and EDX analysis of the prepared Fe_3O_4 MNPs were performed using scanning electronic microscopy (SEM HITACHI SU8220, OXFORD Instruments) that was equipped with an energy dispersive X-ray spectrometry. The crystal phase of the prepared nanoparticles was determined using a PANanalytical EMPYREAN X-ray powder diffraction (XRD) diffractometer (CuK, radiation, $\lambda = 1.541874$ nm), at a scanning speed of 0.07 / min from 15 to 75 (2θ). The surface area and pore size were measured using Brunauer-Emment-Teller (BET) by nitrogen adsorption isotherm at 77.350 K in Micromeritics (ASAP2020, Georgia, and USA). The magnetic properties were analysed using vibrating sample magnetometer (VSM LakeShore 7400 series, Tokyo, Japan). A thermogravimetric analyzer (Perkin Elmer, TGA 4000, Waltham, MA, USA) was used to study the thermal behavior of the prepared adsorbents at temperatures ranging from 30 ^oC to 900 ^oC with a heating rate of 20 ^oC min^{-1} under nitrogen flow. Adsorption studies of CBB G 250 dye were performed using UV spectrophotometer (Shimmadzu, Kyoto, Japan) at a wavelength of 590 nm.

Synthesis of Fe_3O_4 MNPs

The preparation of Fe_3O_4 MNPs were adapted from work published by Zarei et al. [11]. Briefly, 3.1736 g of $FeCl_2.4H_2O$ and 7.5709 g of $FeCl_3.6H_2O$ were dissolved in 320 mL deionized water. The solution was agitated for 1 hour at 80 ^oC. 40 mL of aqueous ammonia was then added slowly into the reaction mixture and was further agitated for another 1 hour before allowed to cool to room temperature. The obtained Fe_3O_4 MNPs were magnetically collected and rinsed five times with hot water until the filtrate turned neutral. Figure 1 depicts the schematic synthesis of Fe_3O_4 MNPs.

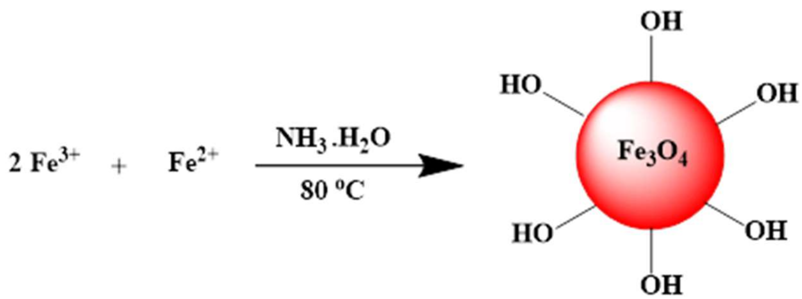

Figure 1. Schematic illustration of synthesis Fe_3O_4 MNPs

Batch adsorption studies

The batch adsorption of CBB G 250 dye from water using Fe_3O_4 MNPs is illustrated in Figure 2. İn this experiment, a quantity of Fe_3O_4 MNPs was added to 10 mL of 50 ppm CBB G 250 dye solution in 50 mL centrifuge tube at room temperature. 0.1 M NaOH and 0.1 M HCl were used to alter the pH of the solution. The solutions were shaken and stirred in an incubator shaker. An external magnet was used to isolate the Fe_3O_4 MNPs from the sample solution. In this experiment, several parameters were studied, such as: 1] adsorbent dosage (0.02–0.14 g), 2] contact time (5-20 min), 3] initial concentrations of CBB G 250 dye (25-100 ppm), and 4] pH of the solutions (3-9) [3]. The concentration of the treated dye in the clear filtrate was determined using an UV spectrophotometer at a wavelength of 590 nm. The removal percentage, (%R) and adsorption capacity (qe) were defined using Equation 1 and Equation 2, respectively [12].

$$R(\%) = \frac{Ci-Ce}{Ci} \times 100\% \tag{1}$$

The equation shown above indicates initial concentration (C_i) and final concentrations (C_e) in ppm of dye ion. Meanwhile,

$$q_e(mg/g) = \frac{C_o-C_e}{m} \times v \tag{2}$$

İn this second equation, q_e denotes adsorption capacity; C_o denotes the initial concentration (ppm); C_e is the final concentration (ppm); m is the adsorbent dosage (g) and v is the volume of working solution.

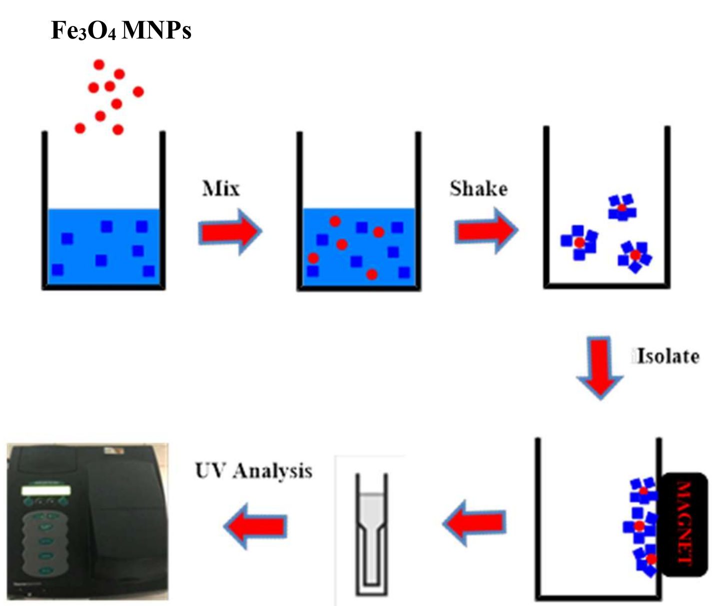

Figure 2. The removal process of CBB G 250 dye using Fe_3O_4 MNPs

Results and Discussion

Characterization

The investigation of FTIRs in the produced Fe3O4 MNPs was performed to examine the functional groups. and the result is illustrated in Figure 3(a). The peak at 537 cm^{-1} in the FTIR spectrum represents the Fe-O band vibration. The two peaks at 3400 and 1604 cm^{-1} adsorption are equivalent to O-H stretching and bending respectively, on the Fe_3O_4 MNPs surface [13]. XRD were used to determine the crystal phases of the prepared Fe_3O_4 MNPs (Figure 3(b)). The spectrum of Fe3O4 MNPs showed the presence of diffraction peaks at 2θ=30.42°, 35.59°, 43.42°, 53.63°, 57.35°, and 63.02° and are respectively assigned to the (220), (311), (400), (422), (511), and (440) planes of Fe_3O_4 (JCPDS 88-O4 0866). These peaks indicate that Fe_3O_4 MNPs has a cubic spinel structure [14].

The magnetic behavior of the Fe_3O_4MNPs was investigated using vibration sample magnetometry (VSM) at room temperature. As observed in Figure 3(c), the superparamagnetic behavior of Fe_3O_4 MNPs indicates a remanence characteristic and a coercivity near to zero. The result of the VSM demonstrates that Fe_3O_4 MNPs have a 63.30 emu g-1 saturation magnetization. The result suggests that manufactured Fe_3O_4 MNPs can be easily collected with an external magnet in water solution (see photo inset of Figure 3(c)). Following this, an analysis was done to study the surface area of Fe_3O_4 MNPs in nitrogen adsorption/desorption (Figure 3(d)). The result shows the specific surface area of Fe_3O_4 MNPs is 123.5 m^2 g^{-1}. It depicts that Fe_3O_4 MNPs have high surface area, suggesting this adsorbent as a good adsorbing agent of organic dyes, particularly CBB G 250 [15].

In order to identify thermal stability of Fe_3O_4 MNPs, thermogravimetric analysis (TGA) was carried out. Thermogram of Fe_3O_4MNPs is presented in Figure 3(e). The finding shows that adsorbed water and hydroxyl group (6.25 %) were lost at temperature below 100 °C. At temperature between 260 and 540 °C, the weight loss of approximately 2.09 % was recorded as a result of change from magnetite (Fe_3O_4) to maghemite (Ɣ-Fe_2O_3) in crystal phase [16].

FESEM analysis was used to investigate the morphology of prepared Fe_3O_4 MNPs. The FESEM images of synthesized Fe_3O_4 MNPs is shown in Figure 4 ((A)-(B)). Fe_3O_4 MNPs were observed in nano-sized, spherical in shape, and have a uniformly distributed particle size [17]. The elemental analysis was performed to confirm the composition of the Fe_3O_4 MNPs and the EDX spectrum of Fe_3O_4 MNPs is shown in Figure 4(C). The EDX results revealed 24.50% Fe and 75.50% of O [18], thus confirming the successful synthesis of the Fe_3O_4 MNPs.

The optimization of the parameter for CBB G dye removal: Effect of adsorbent dosage

The amount of adsorbent is crucial to achieve the maximum removal of CBB G 250 dye. Seven different amounts of Fe_3O_4 MNPs (0.02-0.14g) were used for the adsorption of CBB G 250 dye. Figure 5(a) displays the influence of the adsorbent mass on the removal of target CBB G 250 dye. As seen from the result, as the mass of Fe_3O_4 MNPs increases, so did its adsorption efficiency due to initial availability of the large number of active sites on Fe_3O_4 MNPs [19]. The maximum percentage removal of targeted dye was found at 0.12g of Fe_3O_4 MNPs. Beyond the 0.12g dosage, the adsorption efficiency of Fe_3O_4 MNPs reached equilibrium. This indicates that the active site of the Fe_3O_4 MNPs had become saturated [20]. Consequently, 0.12g was selected for the subsequent experiments.

Effect of contact time

The maximal adsorption of CBB G 250 requires sufficient contact time. The time profile for adsorption was explored by varying the time between 5 and 20 minutes of adsorption. The adsorption recoveries of CBB G 250 increased for up to 15 minutes, after which it plateaued (Figure 5(b)), thus no longer actively absorbing. This is because initially, there are many accessible sites for interaction of CBB G 250 dye which readily allows adsorption. However, as time progresses, more active sites are occupied, which leads to the saturation of the active site on the Fe_3O_4 MNPs becoming saturated after 15 minutes. Hence, 15 minutes of contact time was chosen for future experiments.

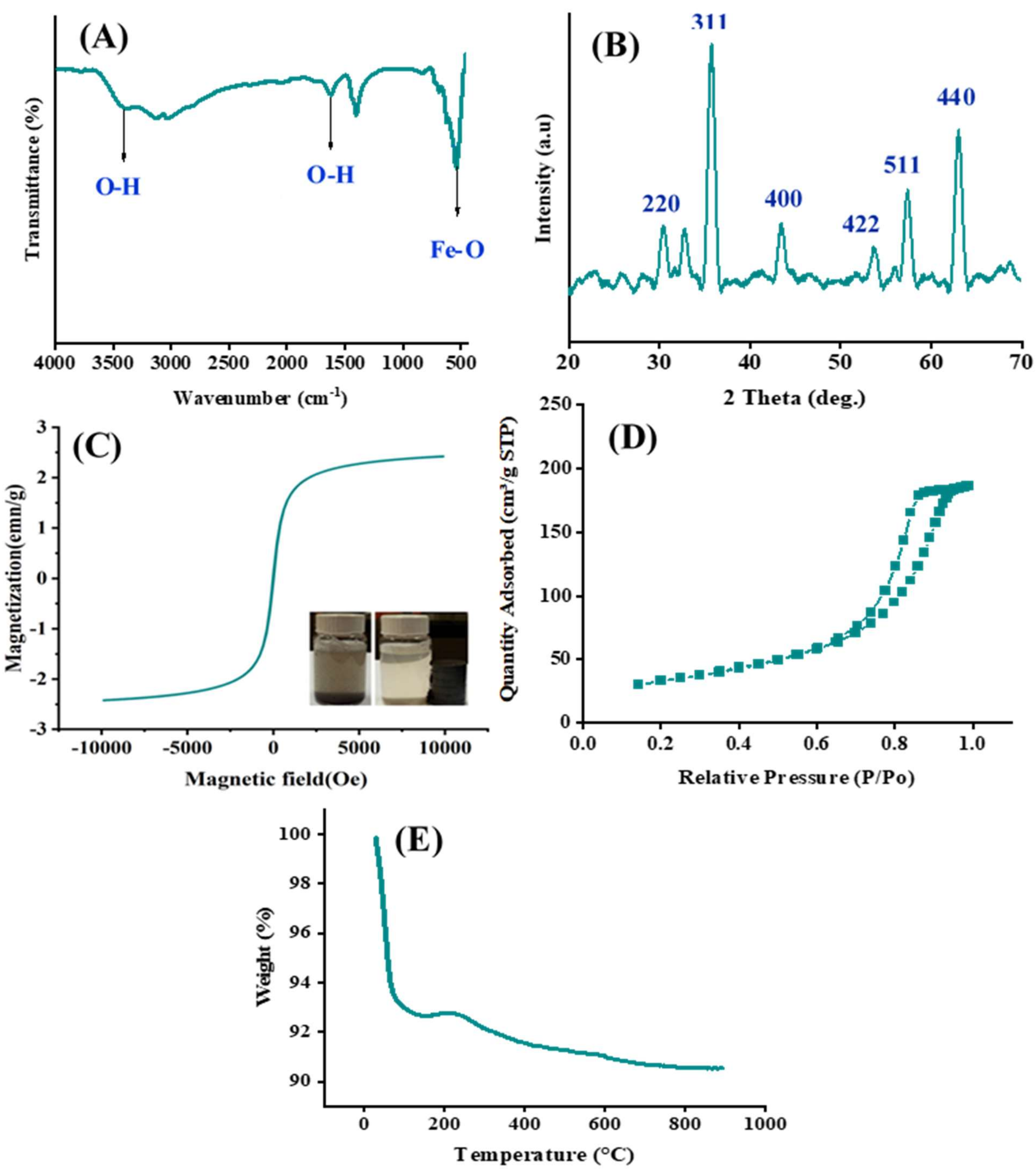

Figure 3. (a) FTIR, (b) XRD, (c) VSM, (d) BET and (e) TGA analyses of Fe_3O_4 MNPs

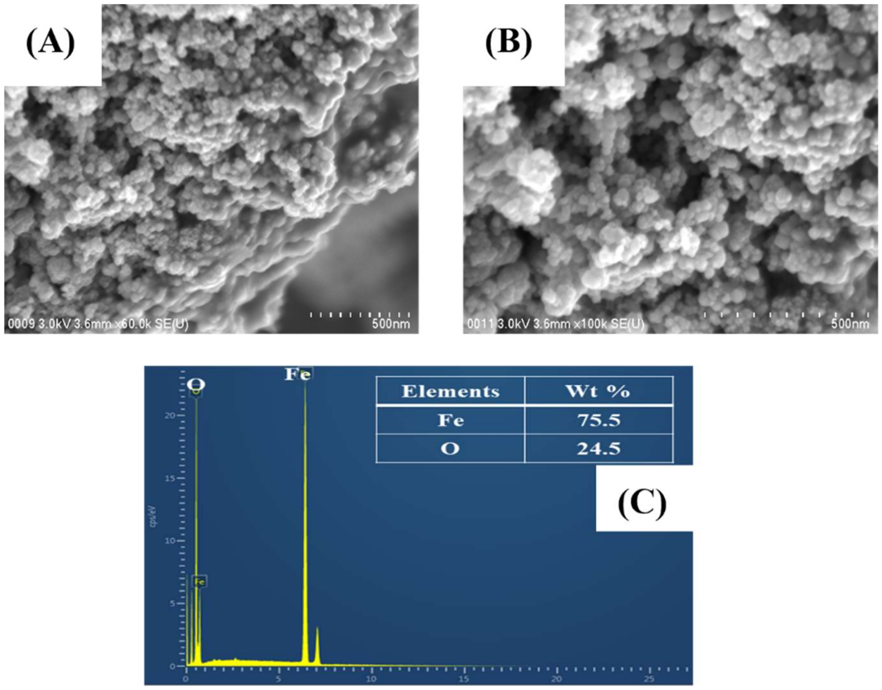

Figure 4. (a-b) Morphological image and (c) EDX spectrum of Fe_3O_4 MNPs

Effect of initial concentration

A suitable concentration of CBB G250 dye is important to achieve a better adsorption efficacy of targeted dye on Fe_3O_4 MNPs. The initial concentrations of CBB G 250 dye ranged from 25 to 100 ppm. Figure 5(c) shows an increasing trend up until 50 ppm of initial dye concentration, suggesting that there are unoccupied active sites on the Fe_3O_4 MNPs adsorbent surface at this stage. The maximum adsorption removal (92%) of targeted dye using Fe_3O_4 MNPs was found at 50 ppm of initial concentration. Beyond this point, the adsorption efficiency of CBB G 250 using Fe_3O_4 MNPs decreases due to the saturation of adsorption sites on the adsorbent surface. This finding agrees with the research conducted by Pandey et al. [21], who reported that the percentage adsorption of Brilliant Green (BG) dye removal decreases with the rise in BG dye concentration. Pandey and coworkers also reported that with the rise in BG dye concentration, the surface area and active sites of the adsorbent became saturated, which then reduces the percentage adsorption of BG. Hence, 50 ppm of initial CBB G 250 concentration was selected for subsequent studies.

Effect of pH

The adsorbent's efficacy is significantly influenced the surface load of the adsorbent material, its ionizing nature of target analytes and the ionization/dissociation of the adsorbed molecules functional groups. Based on Figure 5(d), the high removal of CBB G 250 more than 80% was obtained from pH 3 until pH 10. This phenomenon can be explained based on the structure of CBB G 250 dye and Fe_3O_4 MNPs. Betancur Jiang et al. [22] revealed that Fe_3O_4 MNPs is electropositive for pH $<$ 6 and electronegative for pH $>$ 6.5 which meant that the isoelectric point of Fe_3O_4 MNPs falls between pH 6 and 6.5. Therefore, under acidic conditions, the electropositive Fe_3O_4 MNPs interacted well with the negative charges of the SO_3^- CBB G 250 dye via electrostatic attraction (Figure 6(a)). Meanwhile, under neutral conditions, Fe_3O_4 MNPs adsorbed CBB G 250 dye through hydrogen bonding (Figure 6(b)). Under alkaline conditions, the electronegative Fe_3O_4 MNPs interacted with the positive charges of the N^+ CBB G 250 dye via electrostatic attraction (Figure 6(c)), indicating the good removal of CBB G 250 dye using Fe_3O_4 MNPs at this condition . In this case, pH 8, the natural pH of the sample, is selected as the best pH to use.

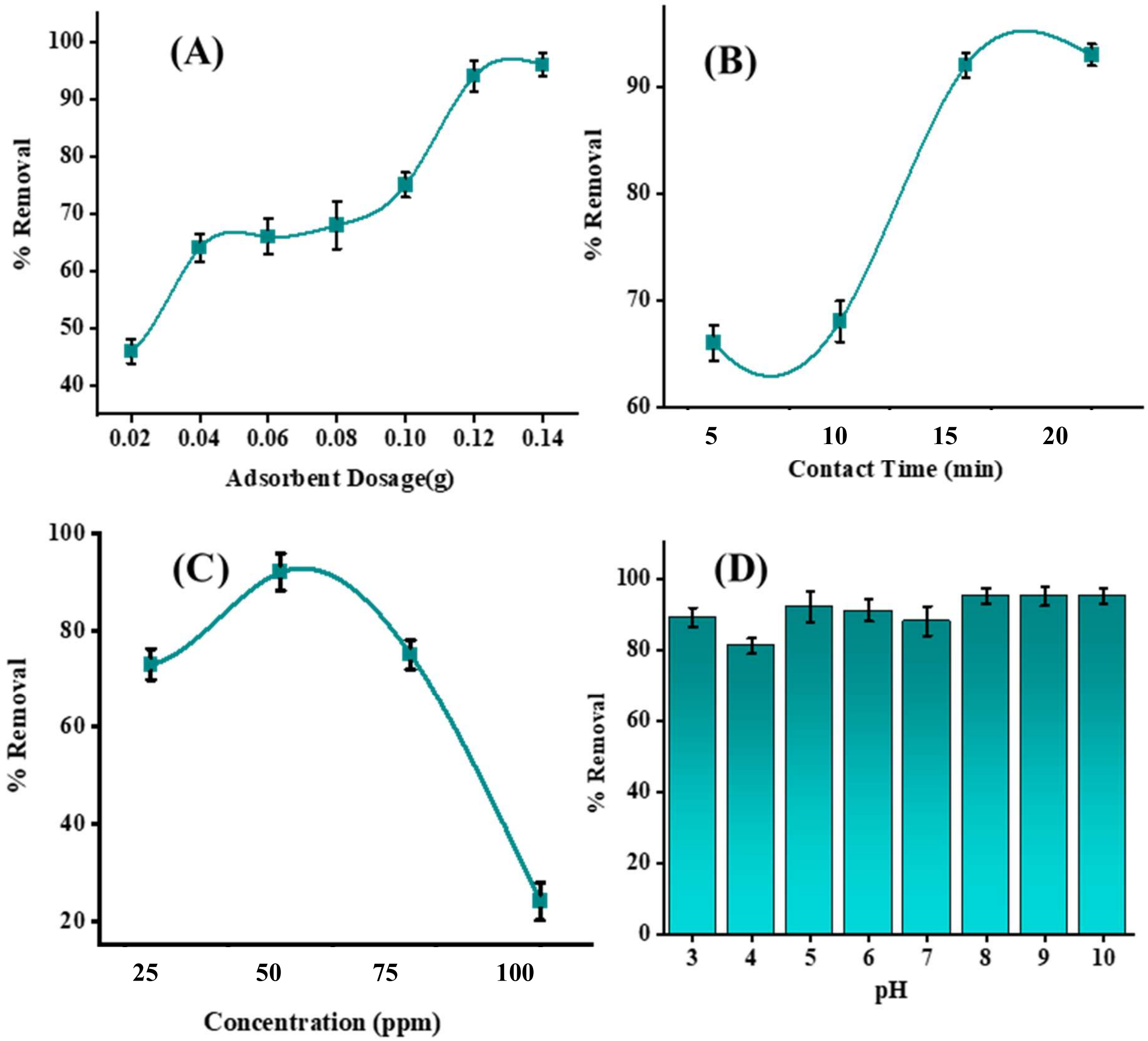

Figure 5. Effect of (a) adsorbent dosage, (b) contact time, and (c) initial concentration; and pH on removal of CBB G 250

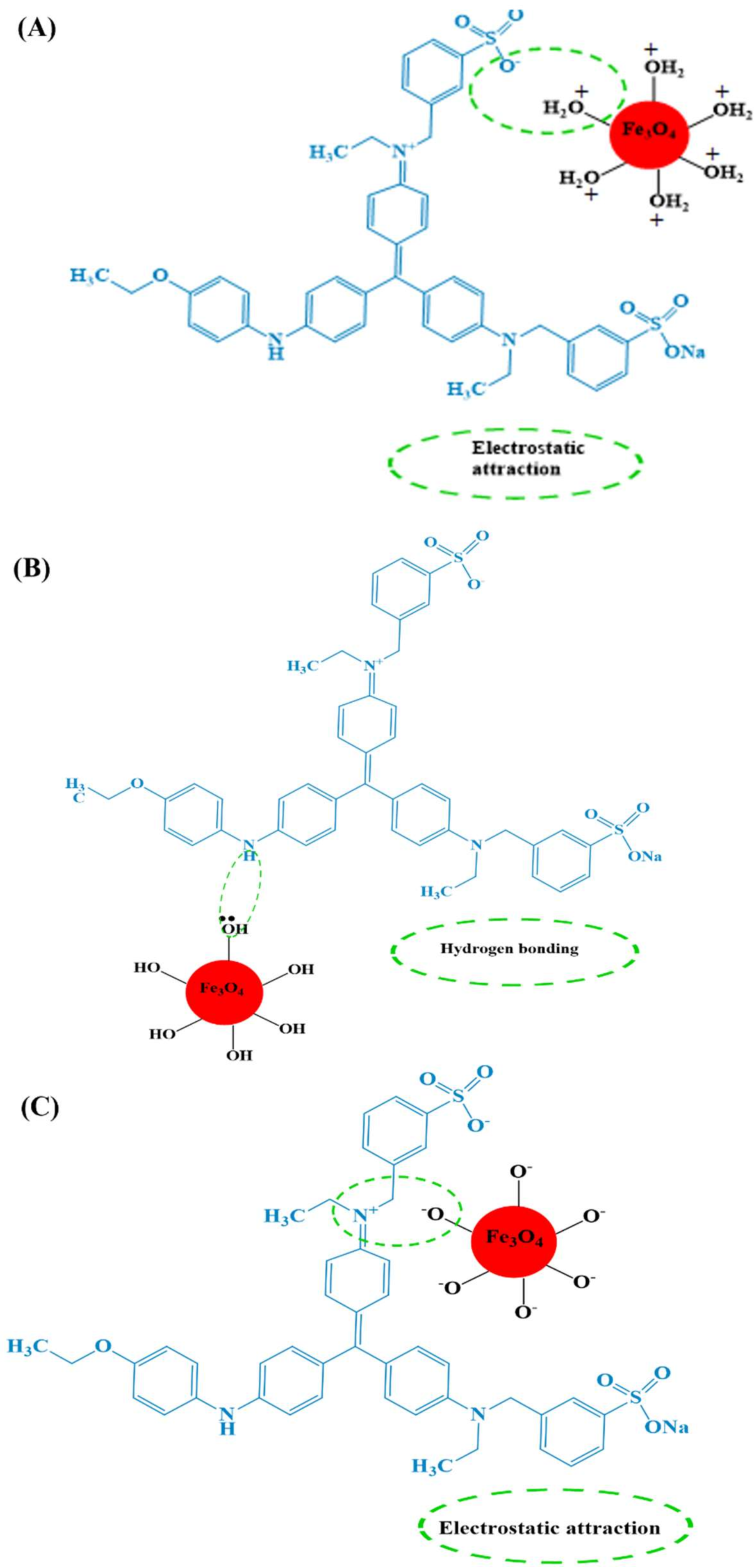

Figure 6. Schematic illustration of adsorption CBB G 250 on Fe_3O_4 MNPs in (a) acidic, (b) neutral and (c) alkaline media

Adsorption kinetic models

The kinetic model delivers a relationship between the rate of adsorption as well as the type of reaction mechanism engaged. To better understand the adsorption mechanism of CBB G 250 dye molecules onto Fe_3O_4 MNPs, the pseudo first-order (Figure 7(a)), pseudo second-order (Figure 7(b)) and intraparticle diffusion (Figure 7 (c)) were used in this study. The kinetic parameters of different models are shown in Table 1. According to this table, the pseudo second-order models fit the experimental data better than that of the pseudo-first-order and the intraparticle diffusion kinetic models, obtaining a correlation coefficient of 0.9507. This indicated that most of the CBB G 250 molecules were adsorbed onto the surface of Fe_3O_4 MNPs by chemisorption mechanism, which involves valence forces via the sharing or exchanging of electrons. Additionally, the adsorption mechanism might depend on both the adsorbate and the adsorbent. The result obtained in this work is similar with the results reported in other published works by Dhananasekaran et al. [23] and Kadeche et al. [24].

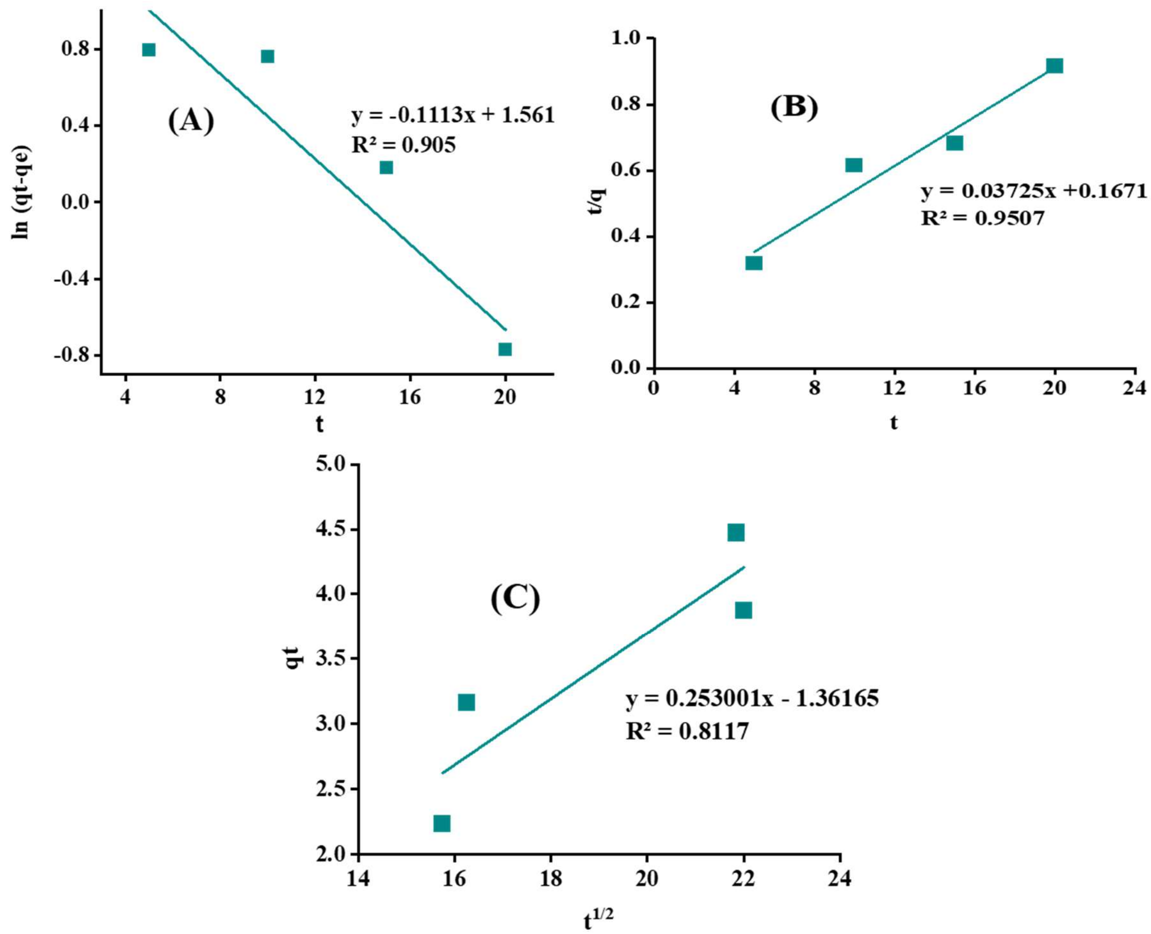

Figure 7. (a) Pseudo-first-order, (b) Pseudo-second-order and (c) Intraparticle Diffusion of removal CBB G 250 by Fe_3O_4 MNPs

Table 1. Kinetic modeling constants and coefficient of determination for adsorption of CBB G 250

Model	Equation /Value
Pseudo-first-order kinetics	$\ln(q_e - q_t) = \ln q_e - k_1 t$
q_e(mg g^{-1})	6.262
R_1^2	0.905
k_1 (min^{-1})	-0.111
Pseudo-second-order kinetics	$\frac{t}{q_1} = \frac{1}{k_2 q_e^2} + \frac{t}{q_e}$
q_e (mg g^{-1})	5.43
R_2^2	0.951
k_2 (g $mg^{-1} min^{-1}$)	0.037
Intraparticle Diffusion	$q_t = k_{id} t^{1/2} + C_i$
R^2	0.957
k_{id} (mg g^{-1} min^{-1})	0.253
Ci (mg g^{-1})	7.939

Adsorption isotherm models

In order to describe further the interaction between the adsorbent and adsorbates, adsorption isotherm models such as Langmuir (Figure 8(a)) and Freundlich (Figure 8(b)) models were studied to fit the equilibrium data. Table 2 shows the adsorption of isotherm constant for CBB G 250 on Fe_3O_4 MNPs. From the table, the high correlation coefficient values for Langmuir ($R^2 = 0.998$) and Freundlich ($R^2 = 0.999$) models strongly imply that the Fe_3O_4 MNPs adsorption of CBB G 250 dye closely follows both Langmuir and Freundlich models of adsorption under the present experimental conditions. This finding is similar to previous study by Kulal & Badalamoole [25] who also found that adsorption of Rhodamine 6G (R6G) dye by Magnetite nanoparticle embedded Pectin-graft-poly (N-hydroxyethylacryl amide) hydrogel followed both Langmuir and Freundlich equations. Othman et al. [26] also stated that the analysis of adsorption of methylene blue using graphene oxide-magnetic iron oxide nanoparticles revealed that the data is well fitted with Langmuir and Freundlich adsorption isotherm model ($R^2 > 0.97$), indicating the multilayer adsorption of dye on the surface of adsorbent.

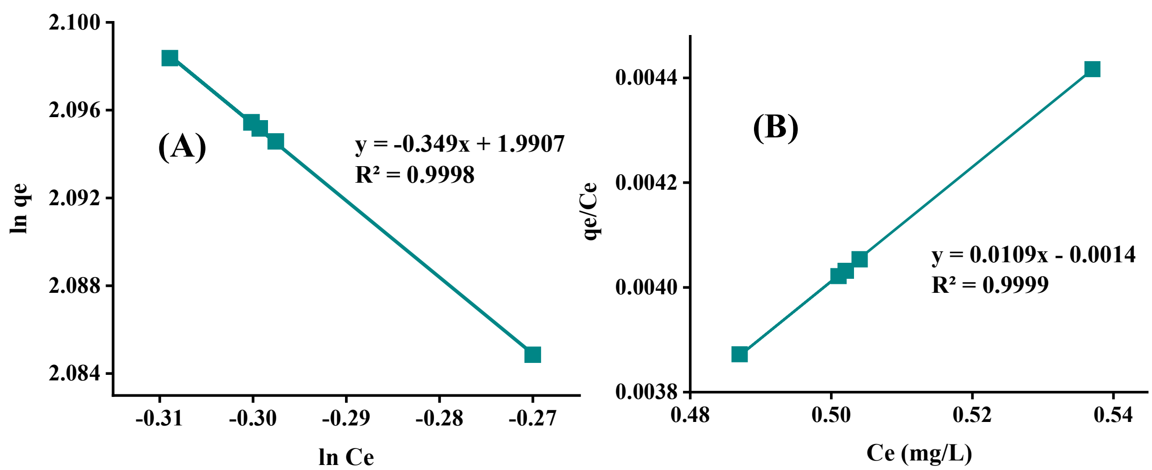

Figure 8. (A) Freundlich adsorption isotherm (B) Langmuir adsorption isotherm of removal CBB G 250 dye by Fe_3O_4 MNPs

Table 2. Isotherm modeling constants and coefficient of determination for adsorption of commassie brilliant blue G 250

Model / Isotherm constant	Equation /Value
Freundlich adsorption isotherm	$\ln q_e = \ln K_F + \frac{1}{n} \ln C_e$
q_e(mg g^{-1})	124.33
R_1^2	0.998
k_F	7.3207
$\frac{1}{n}$	-0.349
Langmuir adsorption isotherm	$\frac{q_e}{C_e} = \frac{C_e}{q_m} + \frac{1}{q_m b}$
q_m (mg g^{-1})	91.743
R_2^2	0.9999

Analysis of CBB G 250 Dye Loaded Fe_3O_4 MNPs

The FTIR spectra of the synthesized Fe_3O_4 MNPs, raw CBB G 250 and CBB G 250 loaded Fe_3O_4 MNPs are shown in Figure 9. From the spectrum of CBB G 250 loaded Fe_3O_4 MNPs, the broad peak at 3439 cm^{-1} is attributed to the overlapping of OH band from Fe_3O_4 MNPs and NH stretching from CBB G 250. Additionally, the peaks at 3179 cm^{-1}, 2052 cm^{-1} and 1063 cm^{-1} suggest the presence of CH stretching and CN stretching, respectively, of CBB G 250. Furthermore, the peak found at 1588 cm^{-1} indicated C=C stretching of CBB G 250. This result proved that CBB G 250 was adsorbed on the surface of Fe_3O_4 MNPs.

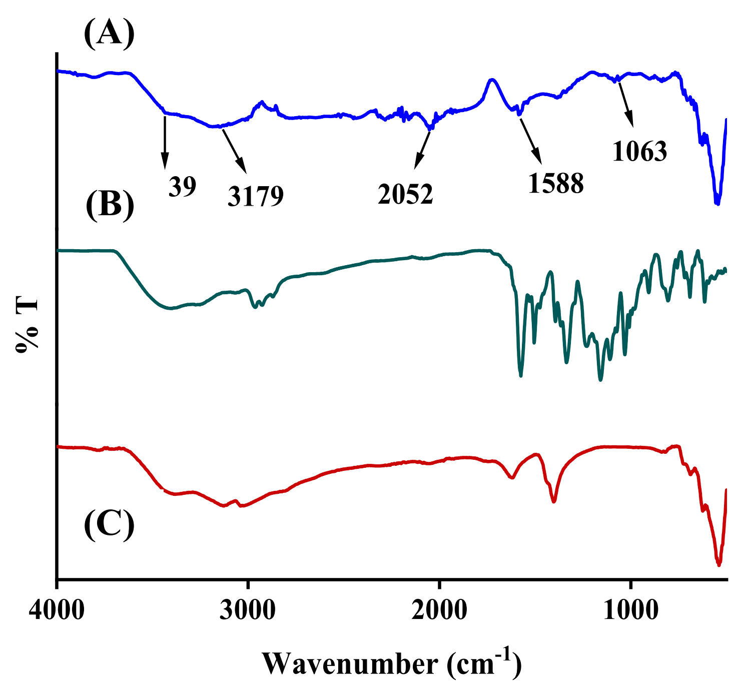

Figure 9. FTIR spectrum of (a) CBB G 250 loaded Fe_3O_4 MNPs (b) CBB G 250 dye (c) Fe_3O_4 MNPs

Recyclability of Fe_3O_4 MNPs

When estimating the efficacy of Fe_3O_4 MNPs in absorbing CBB G 250 in the environment, reusability is a crucial element to take into consideration. Fe_3O_4 MNPs were washed and dried multiple times with ethanol, before being utilized in a second adsorption, to estimate the reusability or adsorption of Fe_3O_4 MNPs. As shown in Figure 10, Fe_3O_4 MNPs can be reused at least six times without any apparent decrease of its efficiency in CBB G 250 removal, suggesting the regeneration efficacy and stability of the prepared adsorbent.

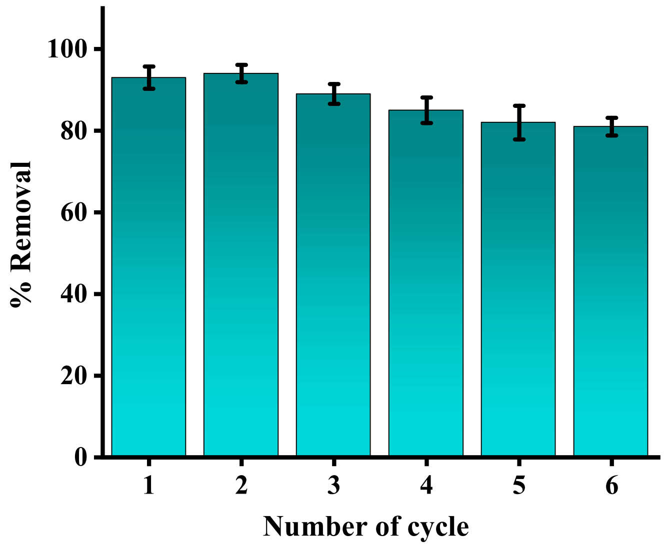

Figure 10. Reusability of Fe_3O_4 MNPs for adsorption efficiency of CBB G 250

Comparison of Fe_3O_4 MNPs with other reported adsorbents for removal of CBB G 250 dye

In Table 3, the present adsorbent, Fe_3O_4 MNPs, was evaluated with previously reported adsorbents for the adsorption of CBB G 250 dye from aqueous environment in terms of amount of adsorbent, contact time, percentage removal, adsorption capacity, kinetic study and isotherm study. The results revealed that proposed Fe_3O_4 MNPs is rapid, reliable, and a highly efficient adsorbent for the treatment of CBB G 250 from water sample. Fe_3O_4 MNPs has the highest adsorption capacity and good percentage removal of CBB G 250 with comparable amount of dosage and contact time as compared to other reported adsorbents.

Conclusion

This present study shows that the synthesized Fe_3O_4 MNPs can be potentially used for the removal of organic dyes from aqueous environment. FESEM, FTIR, and EDX, as well as XRD, TGA, and BET analyses confirmed the successful synthesis of Fe_3O_4 MNPs. Experimental results show that Fe_3O_4 MNPs achieved 95% adsorption at optimum conditions of; 1) 0.12 g dosage, 2) 15 minutes contact time, 3) 50 ppm initial dye concentration, and 4) pH value of 8. The Fe_3O_4 MNPs can also be reused up to six times without losing efficiency. FTIR analysis proved that CBB G 250 dye was adsorbed by Fe_3O_4 MNPs, as evidenced by the intense peaks attributed to the CBB G 250 in the FTIR spectrum. This study demonstrated that Fe_3O_4 MNPs are appropriate for decontamination and treatment of organic contaminants from aqueous environments because they provide excellent magnetic separation, aqueous sample stabilization, high recoveries, and rapid separation.

Table 3. Comparison of the developed adsorbent with other published adsorbents for adsorption of Coomassie brilliant blue dye

Material	Dye	Amount of Adsorbent (g)	Contact Time (min)	Percentage Removal (%)	Adsorption Capacity (mg/g)	Kinetic Study	Isotherm Study	References
Chitin	CBB	0.1	30	65	8.550	Pseudo-second order kinetics	Langmuir isotherm model	[23]
Snail shell powder	CBB	0.02	30	86.3	-	-	Freundlich isotherm model	[2]
Starch/poly(alginicacid-cl-acrylamide) nanohydro- gel (ST/PL(AA-cl-AAm) NHG)	CBB	0.1	150	78.56	31.24	Pseudo-second-order kinetics	Langmuir isotherm model	[27]
α-chitin nanoparticles (CNP)	CBB	0.1	30	98.6	8.550	Pseudo second order kinetics	Langmuir isotherm model	[23]
Activated Carbon from Apricot Stone (ASAC)	CBB	0.1	55		10.09	Pseudo-second order kinetics	Freundlich model	[28]
Sodium bentonite (Bent-Na)	CBB	-	15	85.62	6.848	Pseudo-second order kinetics	Langmuir isotherm model	[24]
Iron-pillared bentonite (PILC-Fe)	CBB	-	15	97.58	9.125	Pseudo-second order kinetics	Langmuir isotherm model	[24]
o-ECNFs	CBB	5.0	300	-	107.80	Elovich model	Redlich-Peterson	[29]
m-ECNFs	CBB	5.0	300	-	46.90	Elovich model	Redlich-Peterson	[29]
Fe_3O_4 MNPs	CBB G 250	0.12	15	95	124.33	Pseudo-second-order model	Langmuir isotherm & Freundlich model	This study

References

1. Verma, R. K., Sankhla, M. S., Rathod, N. V., Sonone, S. S., Parihar, K., and Singh, G. K. (2021). Eradication of fatal textile industrial dyes by wastewater treatment. *Biointerface Research Applied Chemistry*, 12: 567-587.
2. Ibrahim, Hanadi K., Muneer A. Amy, and Eman T. K. (2019). Decolorization of Coomassie brilliant blue G-250 dye using snail shell powder by action of adsorption processes. *Research Journal of Pharmacy and Technology,* 12: 4921-4925.

3. Ezzat, A. O., Tawfeek, A. M., Rajabathar, J. R., and Al-Lohedan, H. A. (2022). Synthesis of new hybrid structured magnetite crosslinked poly ionic liquid for efficient removal of Coomassie brilliant blue R-250 dye in aqueous medium. *Molecules*, 27(2): 441.
4. Nahiun, K. M., Sarker, B., Keya, K. N., Mahir, F. I., Shahida, S., and Khan, R. A. (2021). A review on the methods of industrial wastewater treatment. *Scientific Review*, 7(3): 20-31.
5. Saya, L., Malik, V., Gautam, D., Gambhir, G., Singh, W. R., and Hooda, S. (2022). A comprehensive review on recent advances toward sequestration of levofloxacin antibiotic from wastewater. *Science of The Total Environment*, 813: 152529.
6. Kumar, M., Sridharan, S., Sawarkar, A. D., Shakeel, A., Anerao, P., Mannina, G., ... and Pandey, A. (2022). Current research trends on emerging contaminants pharmaceutical and personal care products (PPCPs): A comprehensive review. *Science of The Total Environment*, 2022: 160031.
7. Jing, G., Meng, X., Sun, W., Kowalczuk, P., and Gao, Z. (2023). Recent advances in treatment and recycling of mineral processing wastewater. *Environmental Science: Water Research & Technology*, 9: 1290-1304.
8. Chai, W. S., Cheun, J. Y., Kumar, P. S., Mubashir, M., Majeed, Z., Banat, F., ... and Show, P. L. (2021). A review on conventional and novel materials towards heavy metal adsorption in wastewater treatment application. *Journal of Cleaner Production*, 296: 126589.
9. Ariffin, M. M., Azmi, A. H. M., Saleh, N. M., Mohamad, S., and Rozi, S. K. M. (2019). Surfactant functionalisation of magnetic nanoparticles: A greener method for parabens determination in water samples by using magnetic solid phase extraction. *Microchemical Journal*, 147(1): 930-940.
10. Ajinkya, N., Yu, X., Kaithal, P., Luo, H., Somani, P., and Ramakrishna, S. (2020). Magnetic iron oxide nanoparticle (IONP) synthesis to applications: present and future. *Materials*, 13(20): 4644.
11. Zarei, A. R., Nedaei, M., and Ghorbanian, S. A. (2018). Ferrofluid of magnetic clay and menthol based deep eutectic solvent: Application in directly suspended droplet microextraction for enrichment of some emerging contaminant explosives in water and soil samples. *Journal of Chromatography A*, 1553: 32-42.
12. Shokry, H., Elkady, M., and Hamad, H. (2019). Nano activated carbon from industrial mine coal as adsorbents for removal of dye from simulated textile wastewater: Operational parameters and mechanism study. *Journal of Materials Research and Technology*, 8(5): 4477-4488.
13. Rozi, S. K. M., Berhanundin, K. M., Ishak, A. R., Mohd, F. L., Rasdi, N. C. D., Rahim, N. Y., ... and Abdullah, A. M. (2023). Novel magnetic eggshell membrane functionalized with waste palm fatty acid for selective adsorption of oil from aqueous solution. *Malaysian Journal of Analytical Sciences*, 27(1): 74-86.
14. Shahriman, M. S., Zain, N. N. M., Mohamad, S., Manan, N. S. A., Yaman, S. M., Asman, S., and Raoov, M. (2018). Polyaniline modified magnetic nanoparticles coated with dicationic ionic liquid for effective removal of rhodamine B (RB) from aqueous solution. *RSC Advances*, 8(58): 33180-33192.
15. Shahriman, M. S., Ramachandran, M. R., Zain, N. N. M., Mohamad, S., Manan, N. S. A., and Yaman, S. M. (2018). Polyaniline-dicationic ionic liquid coated with magnetic nanoparticles composite for magnetic solid phase extraction of polycyclic aromatic hydrocarbons in environmental samples. *Talanta*, 178: 211-221.
16. Bakhshaei, S., Kamboh, M. A., Nodeh, H. R., Zain, S. M., Rozi, S. K. M., Mohamad, S., and Mohialdeen, I. A. M. (2016). Magnetic solid phase extraction of polycyclic aromatic hydrocarbons and chlorophenols based on cyano-ionic liquid functionalized magnetic nanoparticles and their determination by HPLC-DAD. *RSC Advances*, 6(80): 77047-77058.
17. Ahmad, N., Sereshti, H., Mousazadeh, M., Nodeh, H. R., Kamboh, M. A., and Mohamad, S. (2019). New magnetic silica-based hybrid organic-inorganic nanocomposite for the removal of lead(II) and nickel(II) ions from aqueous solutions. *Materials Chemistry and Physics*, 226: 73-81.

18. Yaacob, S. F. F. S., Abd Razak, N. S., Aun, T. T., Rozi, S. K. M., Jamil, A. K. M., and Mohamad, S. (2018). Synthesis and characterizations of magnetic bio-material sporopollenin for the removal of oil from aqueous environment. *Industrial Crops and Products*, 124: 442-448.
19. Yusoff, M. M., Raoov, M., Yahaya, N., and Salleh, N. M. (2017). An ionic liquid loaded magnetically confined polymeric mesoporous adsorbent for extraction of parabens from environmental and cosmetic samples. *RSC Advances*, 7(57): 35832-35844.
20. Yusoff, M. M., Yahaya, N., Saleh, N. M., and Raoov, M. (2018). A study on the removal of propyl, butyl, and benzyl parabens via newly synthesised ionic liquid loaded magnetically confined polymeric mesoporous adsorbent. *RSC Advances*, 8(45): 25617-25635.
21. Pandey, S., Do, J. Y., Kim, J., and Kang, M. (2020). Fast and highly efficient removal of dye from aqueous solution using natural locust bean gum-based hydrogels as adsorbent. *International Journal of Biological Macromolecules*, 143: 60-75.
22. Betancur, J. C., Montoya, P. M., and Calderón, J. A. (2019). Gold recovery from ammonia-thiosulfate leaching solution assisted by PEI-functionalized magnetite nanoparticles. *Hydrometallurgy*, 189: 105128.
23. Dhananasekaran, S., and Palanivel, R. (2015). Adsorption of methylene blue, bromophenol blue and coomassie brilliant adsorption of methylene blue, bromophenol blue and Coomassie brilliant blue by a -chitin nanoparticles. *Journal of Advanced Research*, 7: 113-124.
24. Kadeche, A., Ramdani, A., Adjdir, M., Guendouzi, A., Taleb, S., Kaid, M., and Deratani, A. (2020). Preparation, characterization and application of Fe-pillared bentonite to the removal of Coomassie blue dye from aqueous solutions. *Research on Chemical Intermediates*, 46: 4985-5008.
25. Kulal, P., and Badalamoole, V. (2020). Magnetite nanoparticle embedded Pectin-graft-poly (N-hydroxyethylacrylamide) hydrogel: Evaluation as adsorbent for dyes and heavy metal ions from wastewater. *International Journal of biological macromolecules*, 156: 1408-1417.
26. Othman, N. H., Alias, N. H., Shahruddin, M. Z., Bakar, N. F. A., Him, N. R. N., and Lau, W. J. (2018). Adsorption kinetics of methylene blue dyes onto magnetic graphene oxide. *Journal of Environmental Chemical Engineering*, 6(2): 2803-2811.
27. Sharma, G., Naushad, M., Kumar, A., Rana, S., Sharma, S., Bhatnagar, A., J. Stadler, F., Ghfar, A. A., and Khan, M. R. (2017). Efficient removal of Coomassie brilliant blue R-250 dye using starch/poly (alginic acid-cl-acrylamide) nanohydrogel. *Process Safety and Environmental Protection*, 109: 301-310.
28. Cherfi Abdelhamid, A. M. (2014). Kinetic and equilibrium studies of Coomassie Blue G-250 adsorption on apricot stone activated carbon. *Journal of Environmental & Analytical Toxicology*, 05(2): 1000264.
29. Thamer, B. M., Aldalbahi, A., Moydeen A, M., El-Hamshary, H., Al-Enizi, A. M., and El-Newehy, M. H. (2019). Effective adsorption of Coomassie brilliant blue dye using poly (phenylene diamine) grafted electrospun carbon nanofibers as a novel adsorbent. *Materials Chemistry and Physics*, 234(1): 133-145.